Inorganic Chemistry

Article

pubs.acs.org/IC

Triple Framework Interpenetration and Immobilization of Open Metal Sites within a Microporous Mixed Metal–Organic Framework for Highly Selective Gas Adsorption

Zhangjing Zhang,[†,‡] Shengchang Xiang,*[,†,‡] Kunlun Hong,[⊥] Madhab, C. Das,[†] Hadi D. Arman,[†] Maya Garcia,[§] Jalal U. Mondal,[§] K. Mark Thomas,[∥] and Banglin Chen*[,†]

[†]Department of Chemistry, University of Texas at San Antonio, One UTSA Circle, San Antonio, Texas 78249-069, United States

[‡]College of Chemistry and Materials, Fujian Normal University, 3 Shangsan Road, Cangshang Region, Fuzhou, China 350007

[§]Department of Chemistry, University of Texas–Pan American, 1201 West University Drive, Edinburg, Texas 78541, United States

[⊥]Center for Nanophase Materials Sciences, Oak Ridge National Laboratory, Oak Ridge, Tennessee 37831, United States

[∥]Northern Carbon Research Laboratories, Sir Joseph Swan Institute for Energy Research and School of Chemical Engineering and Advanced Materials, University of Newcastle upon Tyne, Bedson Building, Newcastle upon Tyne, NE1 7RU, U.K.

Supporting Information

ABSTRACT: A three-dimensional triply interpenetrated mixed metal–organic framework, $Zn_2(BBA)_2(CuPyen)\cdot G_x$ (**M'MOF-20**; BBA = biphenyl-4,4′-dicarboxylate; G = guest solvent molecules), of primitive cubic net was obtained through the solvothermal reaction of $Zn(NO_3)_2$, biphenyl-4,4′-dicarboxylic acid, and the salen precursor $Cu(PyenH_2)(NO_3)_2$ by a metallo-ligand approach. The triple framework interpenetration has stabilized the framework in which the activated **M'MOF-20a** displays type-I N_2 gas sorption behavior with a Langmuir surface area of 62 $m^2\ g^{-1}$. The narrow pores of about 3.9 Å and the open metal sites on the pore surfaces within **M'MOF-20a** collaboratively induce its highly selective C_2H_2/CH_4 and CO_2/CH_4 gas separation at ambient temperature.

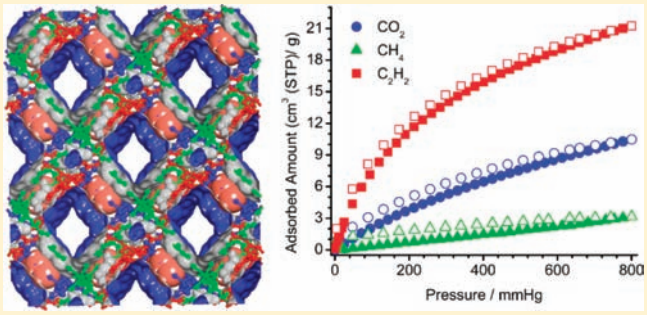

INTRODUCTION

Porous metal–organic framework (MOF) materials are hot research topics among the inorganic and materials science community over the past two decades for their diverse applications in gas storage, separation, sensing, and heterogeneous catalysis.[1−21] In terms of porous MOFs for their gas separation, the subtle tuning of the micropores/channels/windows is very important to maximize their size-exclusive effects in which the small gas molecules can enter through the pore spaces while large gas molecules will be blocked.[11,12] The immobilization of open metal sites and specific functional organic groups on the pore surfaces of MOFs can induce their differential interactions with gas molecules and, thus, has become another very important strategy to enhance gas separation selectivity.[3,4] These two strategies have been realized separately to target porous MOFs for selective gas sorption/separation over the past several years. For example, to make use of two types of organic linkers, bicarboxylates ($R(COO)_2$) and bidentate pillar linkers (L), for the construction of the cubic MOFs $Zn_2(R(COO)_2)_2(L)$ and to introduce framework interpenetration for the tuning of the micropore spaces, a series of microporous MOFs of variable pores, from 3 to 6 Å, have been realized for their selective gas separation,[12] while the immobilization of organic groups such as −OH and $-NH_2$ has been realized as an efficient methodology to induce their different interactions with gas molecules.[3,4,23] The cubic MOF $Zn_2(R(COO)_2)_2(L)$ approach has been very successful to tune the micropores by framework interpenetration; however, it is very difficult to further immobilize functional sites within these traditional MOFs to collaboratively enhance their highly selective gas separation.

The situation might be changed since the realization of the metallo-ligand approach to construct microporous mixed metal–organic frameworks (M'MOFs).[17,18] As shown in Scheme 1, instead of pure organic pillars in the construction of traditional MOFs, metal–organic complexes as the metallo-ligands are utilized to coordinate with the second metal ions/metal clusters to form the M'MOFs. This metallo-ligand approach has logically provided rational strategies to immobilize different open metal sites in porous M'MOFs for their selective gas sorption, as demonstrated in our recent examples of microporous M'MOFs for their selective adsorption of H_2/D_2[18c] and C_2H_2/C_2H_4.[18d] Herein we report the first example of

Received: September 30, 2011
Published: April 23, 2012

 © 2012 American Chemical Society dx.doi.org/10.1021/ic2021275 | *Inorg. Chem.* 2012, 51, 4947–4953

Scheme 1. Metallo-ligand Approach to Construct Mixed Microporous MOFs of Primitive Cubic Nets, Whose Pore Size Can Be Reduced or Rationally Adjusted by Triple Framework Interpenetration

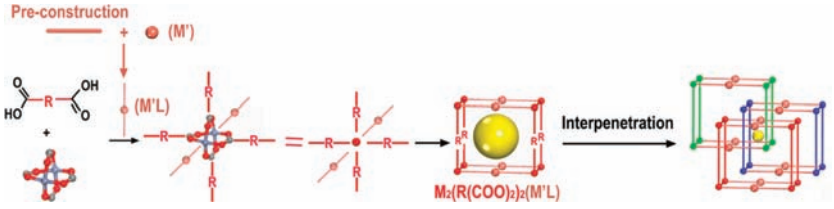

Table 1. Virial Graph Analyses Data for M'MOF-20a and Its CO_2/CH_4 and C_2H_2/CH_4 Separation Selectivities

adsorbate	T/K	K_H/mol g^{-1} Pa^{-1}	A_0/ln(mol g^{-1} Pa^{-1})	A_1/g mol^{-1}	R^2	S_{ij}[a]	S_2	Q_{st}/kJ mol^{-1}
CH_4	273	2.813×10^{-9}	−19.689 ± 0.00204	−666.434 ± 38.594	0.987			24.8
	295	1.209×10^{-9}	−20.533 ± 0.00222	−11.156 ± 4.211	0.951			
CO_2	273	2.147×10^{-8}	−17.657 ± 0.00284	−1491.341 ± 12.471	0.999	7.6		28.4
	295	8.171×10^{-9}	−18.623 ± 0.00273	−1485.832 ± 23.258	0.998	6.8		
C_2H_2	273	1.324×10^{-7}	−15.837 ± 0.0344	−1692.479 ± 5.861	0.999	47.1	6.2	33.7
	295	4.215×10^{-8}	−16.982 ± 0.0022	−1577.320 ± 12.653	0.999	34.9	5.1	

[a]The Henry's law selectivity for gas component *i* over CH_4 at the speculated temperature is calculated based on the equation $S_{ij} = K_H(i)/K_H(CH_4)$. Similarly, S_2 is the Henry's law selectivity for C_2H_2 over CO_2.

microporous M'MOFs, $Zn_2(BBA)_2(CuPyen)\cdot G_x$ (**M'MOF-20**, BBA is biphenyl-4,4′-dicarboxylate), of a primitive cubic net in which the triple framework interpenetration to tune the micropores and immobilization of open copper(II) sites to induce their differential interactions with gas molecules have been collaboratively implemented for highly selective gas adsorption.

EXPERIMENTAL SECTION

Materials and Measurements. All reagents and solvents were used as received from commercial suppliers without further purification. Thermogravimetric analyses (TGA) were performed on a Mettler Toledo TGA/SDTA851 analyzer in air with a heating rate of 5 K min^{-1}, from 30 to 800 °C. X-ray powder diffraction (XRD) patterns were measured using a Bruker D8 Advance powder diffractometer at 40 kV, 40 mA for Cu Kα radiation (λ = 1.5418 Å), with a scan speed of 0.2 s/step and a step size of 0.02° (2θ). 5-Methyl-4-oxo-1,4-dihydropyridine-3-carbaldehyde and the precursor $Cu(PyenH_2)(NO_3)_2$ were synthesized according to the literature procedure.[18d]

Gas Sorption Measurements. A Micromeritics ASAP 2020 surface area analyzer was used to measure gas adsorption. In order to remove guest solvent molecules in the framework, a freshly prepared sample of **M'MOF-20** was activated at 423 K under high vacuum for 12 h until the outgas rate was <5 μmHg min^{-1} prior to measurements. The sorption measurement was maintained at 77 K with liquid nitrogen and at 273 K with an ice−water bath (slush), respectively. As the center-controlled air conditioner was set at 22.0 °C, a water bath of 22.0 °C was used for adsorption isotherms at 295.0 K.

Virial Graph Analyses. Isotherm data were analyzed using the virial equation[18]

$$\ln(n/P) = A_0 + A_1 n + A_2 n^2 + \ldots$$

where p is pressure, n is the amount adsorbed, and A_0, A_1, etc., are virial coefficients. A_0 is related to adsorbate−adsorbent interactions, whereas A_1 describes adsorbate−adsorbate interactions. The Henry's law constant (K_H) is equal to $\exp(A_0)$, and the selectivity can be obtained from the constant K_H. The virial parameters are given in Table 1.

Zero Surface Coverage. The isosteric enthalpies of adsorption at zero surface coverage ($Q_{st,n=0}$) are a fundamental measure of adsorbate−adsorbent interactions, and these values were obtained from the A_0 values obtained by extrapolation of the virial graph to zero surface coverage.

Van't Hoff Isochore. The isosteric enthalpies of adsorption as a function of surface coverage were calculated from the isotherms using the van't Hoff isochore, which is given by the following equation.

$$\ln(p) = -\frac{\Delta H}{RT} + \frac{\Delta S}{R}$$

A graph of ln$P$ versus $1/T$ at constant amount adsorbed (n) allows the isosteric enthalpy and entropy of adsorption to be determined. The pressure values for a specific amount adsorbed were calculated from the adsorption isotherms by the following methods: (1) assuming a linear relationship between adjacent isotherm points starting from the first isotherm point, (2) using the virial equation at low surface coverage. The agreement of the results from the two methods can help us to confirm the reliability of the isosteric enthalpies and the Henry's law selectivities from the virial fit for gas adsorption on the porous MOFs.

Synthesis of $Zn_2(BBA)_2[Cu(Pyen)]\cdot 3DMF\cdot H_2O$ (M'MOF-20). A mixture of $Zn(NO_3)_2\cdot 6H_2O$ (19.8 mg, 0.07 mmol), H_2BBA (14.6 mg, 0.05 mmol), and $Cu(PyenH_2)(NO_3)_2$ (9.8 mg, 0.02 mmol) was dissolved in the mixed solution of 5 mL of DMF and 1 mL of H_2O and heated in a vial (23 mL) at 80 °C for 24 h. The dark blue thin plates formed were collected and dried in the air (13 mg, 53%). Anal. Calcd for $Zn_2(BBA)_2[Cu(Pyen)]\cdot 3DMF\cdot H_2O$ ($C_{53}H_{55}N_7O_{14}CuZn_2$): C: 52.68; H: 4.59; N: 8.11. Found: C: 52.39; H: 4.48; N: 8.20.

Single-Crystal X-ray Structure Determination. The intensity data sets of **M'MOF-20** were collected on a Rigaku Saturn724 diffractometer equipped with graphite-monochromated Mo Kα radiation (λ = 0.71073 Å) using an ω-scan technique at 173 K. The data set was reduced by CrystalClear and CrystalStructure programs.[19] The structure was solved by direct methods and refined using the SHELXTL software package. The H atoms on the ligand were placed in idealized positions and refined using a riding model. The solvent of DMF could not be located; we employed PLATON/SQUEEZE to calculate the diffraction contribution of the solvent molecules, thereby producing a set of solvent-free diffraction intensities.[20] CCDC-831797 contains the supplementary crystallographic data for **M'MOF-20**. The data can be obtained free of charge from The Cambridge Crystallographic Data Centre via www.ccdc.cam.ac.uk/data_request/cif.

RESULTS AND DISCUSSION

The framework of **M'MOF-20** is composed of paddle wheel dinuclear zinc carboxylate units $\{Zn_2(COO)_4\}$, which are bridged by the BBA ligands to form a distorted 2D square grid

dx.doi.org/10.1021/ic2021275 | Inorg. Chem. 2012, 51, 4947−4953

(Figure 1). The 2D square grids are diagonally pillared by Cu(Pyen) metallo-liangds, whose nitrogen atoms occupy the

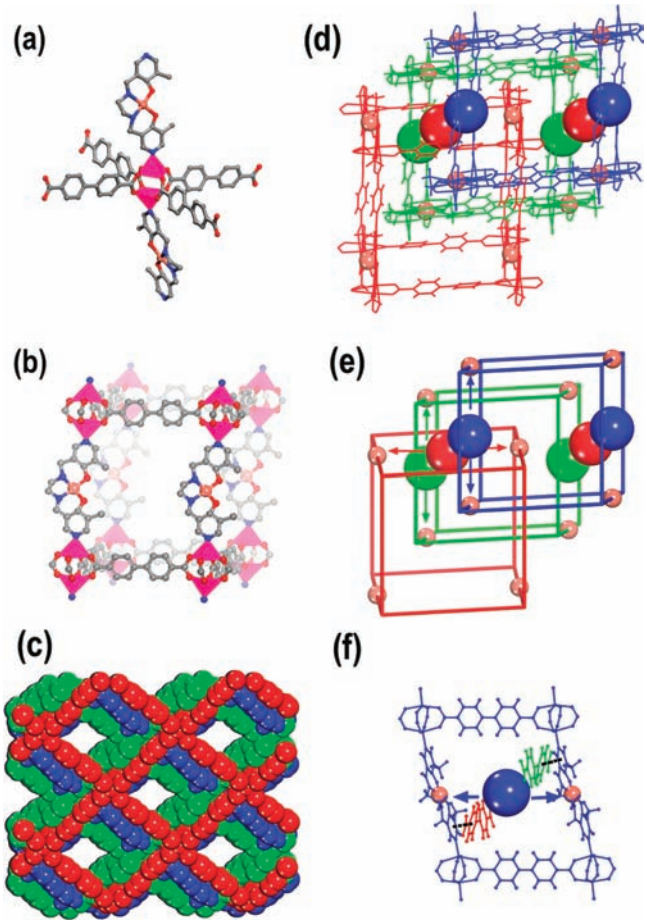

Figure 1. Structure of **M'MOF-20**. The paddle wheel $\{Zn_2(COO)_4\}$ node linked by four BBA and two Cu(Pyen) units (a) to form a single network with a rhombohedral cage (b) (carbon, gray; oxygen, red; nitrogen, blue; copper, maroon). (c) Space-filling diagram showing network interpenetration with a 1D channel of 3.9 Å along the *c* direction. Crystal structure (d) and perspective views (e) of a triply interpenetrated network with immobilized open Cu^{2+} sites, showing the cavity situated in the face center of each rhombohedral cage (Cu, maroon ball; cavity centers, red, green, and blue balls). (f) Face of the rhombohedral cage showing the cavity environment and the $\pi-\pi$ interactions (black dash) between the pyridine ring of the salen pillar and the benzene ring of the BBA group from an identical network.

axial sites of the $\{Zn_2(COO)_4\}$ paddle wheels, to form a 3D framework with a topology that can be described as an elongated primitive cubic lattice. The rhombohedral cage in a single primitive cubic net has the dimensions 20.4 × 22.6 Å, 20.6 × 21.7 Å, and 18.3 × 23.7 Å in the *c*, *a*, and *b* directions, respectively (Figure 1b). The spacious nature of the single network allows two other identical networks to penetrate it in a normal mode, thus resulting in a triply interpenetrating array (Figure 1c). Because of the triple framework interpenetration, the channel in the crystallographic *b* and *a* directions is essentially blocked, leaving rhombic channels in the *c* direction with a side length of about 3.9 Å. Solvent occupies 29.9% of the volume of **M'MOF-20** as determined by PLATON.[20]

It is very important to point out that all Cu sites are still accessible to the channels after the framework interpenetration, as shown in Figure 1e,f. The cavity is centered at the Wyckoff position *4a* (0, 0, 0), one of the face centers of each rhombohedral cage. After the interpenetration, two BBA units from the two identical networks stand perpendicular to the two salen pillars in one-to-one fashion, which seems to be driven by the intermolecular $\pi-\pi$ interactions between one benzene ring from the BBA unit and the pyridine group from the salen held at a centroid−centroid distance of 3.593 Å. The dihedral angle between the benzene and pyridine groups is 5.6°. Although the BBA groups lie between the cavity and the salen pillars, the $\pi-\pi$ interactions between the identical networks effectually keep the framework stable and prevent the BBA groups from overriding the Cu sites. The triple interpenetration not only makes the channels smaller but also leads to the shortest distance between Cu ions on different networks of 7.8 Å.

The interpenetration is expected to stabilize the framework; we thus examined the permanent porosity of **M'MOF-20** in detail. Methanol-exchanged **M'MOF-20** was activated at room temperature under high vacuum to obtain the activated sample **M'MOF-20a**. The N_2 sorption isotherm of **M'MOF-20a** (Figure 2) at 77 K indicates a typical type I behavior with a

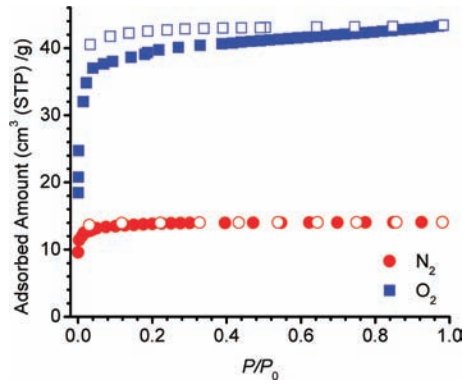

Figure 2. Adsorption isotherms of N_2 (red circle) and O_2 (blue square) gases on **M'MOF-20a** at 77 K.

Langmuir (BET) surface area of 62 $m^2\ g^{-1}$ (42 $m^2\ g^{-1}$). The adsorbed amount of N_2 is 13.6 $cm^3\ g^{-1}$ (STP), while **M'MOF-20a** can take O_2 of 43.4 $cm^3\ g^{-1}$, 3.2 times the N_2 uptake, at P/P_0 = 1 and 77 K. The hydrogen adsorption isotherm (Figure S1) indicates an uptake of 40 $cm^3\ g^{-1}$ (0.4 wt %) at 77 K and 1 atm. The total pore volumes were calculated from the highest measured values using densities of 0.071, 0.809, and 1.141 g cm^{-3} for the liquid densities of H_2, N_2, and O_2, respectively.[21] The total pores volumes were 0.052, 0.022, and 0.054 $cm^3\ g^{-1}$ for H_2, N_2, and O_2, respectively. The values for the small H_2 (size 240 × 240 × 314 pm)[18d] and O_2 (size 293.0 × 298.5 × 405.2 pm)[22] probe are consistent, more than twice that for the large N_2 probe. After the triple interpenetration, at least half of the pore space in **M'MOF-20a** is too small to accommodate the slightly large N_2 gas (size 299.1 × 305.4 × 404.6 pm).[22]

The small micropores and pore volume enabled us to examine the potential application of **M'MOF-20a** for the industrially important C_2H_2/CH_4 and CO_2/CH_4 separations.[23−25] Interest in separating acetylene from methane mixtures comes from two considerations: (1) acetylene is principally derived from the cracking of natural gas, during which purification is necessary to meet the requirement of grade A acetylene for organic synthesis;[26] (2) significant problems are created as a result of acetylene solidification in hydrocarbon separation systems.[27] Acetaldehyde as a selective

dx.doi.org/10.1021/ic2021275 | Inorg. Chem. 2012, 51, 4947−4953

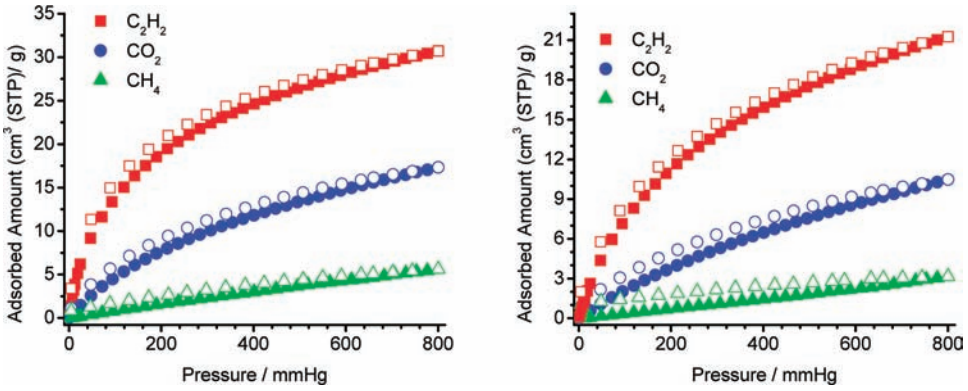

Figure 3. Adsorption (solid) and desorption (open) isotherms of acetylene (red squares), carbon dioxide (blue circles), and methane (green triangles) on **M'MOF-20a** at 273 K (left) and 295 K (right).

solvent[28] or some adsorbents such as ammonium molybdophosphate[29] and SBA-15[30] have been employed for the separation of C_2H_2 from CH_4. As shown in Figure 3, **M'MOF-20a** takes up acetylene of 21 $cm^3\ g^{-1}$ and carbon dioxide of 10 $cm^3\ g^{-1}$, respectively, 7.2 and 3.4 times the value of methane (2.9 $cm^3\ g^{-1}$) at 295 K and 1 atm, highlighting **M'MOF-20a** as a promising material for the highly selective separation of C_2H_2/CH_4 and CO_2/CH_4 at room temperature. The total pore volumes were calculated from the highest measured values at 273 K using densities of 0.423, 1.032, and 0.729 g cm^{-3} for the densities of CH_4, CO_2, and C_2H_2, respectively.[21] The liquid densities were used for both CH_4 and CO_2, while the only available density for C_2H_2 was for solid C_2H_2. The total pore volumes are 0.009, 0.033, and 0.049 $cm^3\ g^{-1}$ for CH_4, CO_2, and C_2H_2, respectively. The pore volume from C_2H_2 uptake is close to that from the saturated O_2 uptake, taking the latter as the benchmark, showing acetylene almost occupies the pore of **M'MOF-20a** even at 273 K. The total pore volume calculated from the CH_4 uptake at 295 K is 0.005, 9% of the benchmark, indicating that only very few CH_4 molecules enter into **M'MOF-20a**. Such low methane uptakes are attributed to both weak interactions of methane molecules with the pore surface and the larger molecular dimensions of methane. The dimensions of methane (382.9 × 394.2 × 410.1 pm)[22] with a tetrahedral shape are more than the side length of the rhombic channels of **M'MOF-20a**, which might restrict the access of methane molecules into the pores. In comparison, the sizes of C_2H_2 (332 × 334 × 570 pm)[22] and CO_2 (318.9 × 333.9 × 536.1 pm)[22] are small enough to readily enter the rhombic channels of **M'MOF-20a**.

In order to establish why **M'MOF-20a** exhibits such a high selective separation for C_2H_2/CH_4 and CO_2/CH_4, its coverage-dependent adsorption enthalpies of acetylene, methane, and CO_2 were calculated on the basis of the virial method and the van't Hoff isochore. The virial graphs for adsorption of CH_4, C_2H_2, and CO_2 on **M'MOF-20a** at 273 and 295 K are shown in supplementary Figures S2–S4. It is apparent that the virial graphs have very good linearity in the low-pressure region. The parameters and the enthalpies obtained from the virial equation are summarized in Table 1. The values of the first virial coefficient (A_0) reflect adsorbate/adsorbent interaction, whereas the second virial parameter (A_1) is a function of adsorbate/adsorbate interactions. Typical values of A_1 for adsorption of gases and vapors on carbon molecular sieves have been reported in the range ~−0 to −5000 g mol^{-1}.[22,31] The A_1 virial parameters for methane increase from −666 to −11 g mol^{-1} from 273 to 295 K, which also has a similar trend, but with more drastic change of A_1 values on a carbon molecular sieve, increasing from −986 to −899 g mol^{-1} from 303 to 343 K.[31] The small A_1 value of methane on **M'MOF-20a** at 295 K also indicates that very little methane is captured by the adsorbent under this condition. The A_1 virial parameters for acetylene (−1692 to −1577 g mol^{-1}) on **M'MOF-20a** are comparable with those on **M'MOF-2a** ($Zn_3(BDC)_3[Cu(SalPycy)]$, −1621 to −1353 g mol^{-1}), **M'MOF-3a** ($Zn_3(CDC)_3[Cu(SalPycy)]$, −2057 to −1693 g mol^{-1}),[18c] and a carbon molecular sieve (−1444 to −1302 g mol^{-1}).[22] The trends in the A_1 parameters for CH_4 and C_2H_2 adsorption on **M'MOF-20a** are consistent with the adsorbate–adsorbate interactions decreasing with increasing temperature. The A_1 values for CO_2 adsorption on **M'MOF-20a** are similar at −1491 g mol^{-1}, showing that the adsorbate–adsorbate interactions might be independent of temperature from 273 to 295 K, but it is apparent that the viral parameters have similar values to those on **M'MOF-2a** (−1071 to −940 g mol^{-1})[18c] and the carbon molecular sieve (−1000 to −1045 g mol^{-1}).[22] Comparison of H_2 and D_2 adsorption on **M'MOF-1**[18d] and carbon molecular sieves[18e] shows that A_1 values for D_2 are less negative than the corresponding values for H_2. The differences in A_1 indicate higher repulsion energies between neighbors for H_2 than for D_2. This is related to the larger zero-point energy of H_2 compared with D_2. **M'MOF-3a** has smaller pores compared to **M'MOF-20a**, as shown by no N_2 adsorption at 77 K. Adsorption of CO_2 on **M'MOF-3a** has higher repulsive interactions (−3117 to −1903 g mol^{-1}) compared with **M'MOF-20a** due to confinement in smaller ultramicroporosity.[18c]

The isosteric enthalpies of adsorption ($Q_{st,n=0}$) at zero surface coverage were 24.8, 28.4, and 33.7 kJ mol^{-1} for CH_4, CO_2, and C_2H_2 adsorption on **M'MOF-20a** over the temperature range 273–295 K. Although the enthalpy for CO_2 is lower than the extra high ones on MIL-100 (60 kJ mol^{-1})[32] and HCu-$[(Cu_4Cl)_3(BTTri)_8(en)_5]$ (90 kJ mol^{-1}),[33] it is even slightly higher than those on some MOFs with the same open Cu^{2+} sites (26, 23, and 21 kJ mol^{-1} respectively for HKUST-1,[24d] PCN-11,[24d] and $HCu[(Cu_4Cl)_3(BTTri)_8]$).[33] The enthalpies for the threes gases on **M'MOF-20a** are systematically higher than those found in MIL-53, with larger pores,[15h] and even higher than those found in some MOFs with open Zn^{2+} sites (18.3, 24.4, and 24.0 kJ mol^{-1} respectively for CH_4, CO_2, and C_2H_2 on Zn-MOF-74[14c,f,h] and 14.8, 20.2, and 28.2 kJ mol^{-1} on $[Zn_4(OH)_2(1,2,4\text{-BTC})_2]$[23c]). Apparently, both the accessible Cu^{2+} sites and the narrow pores within **M'MOF-20a** contribute

dx.doi.org/10.1021/ic2021275 | Inorg. Chem. 2012, 51, 4947–4953

to the stronger interactions with the gas molecules. The comparison of the results from the two methods, the linear extrapolation and the virial equation, shows that there is a very good agreement (Figure 4). In the cases of C_2H_2 and CH_4, the

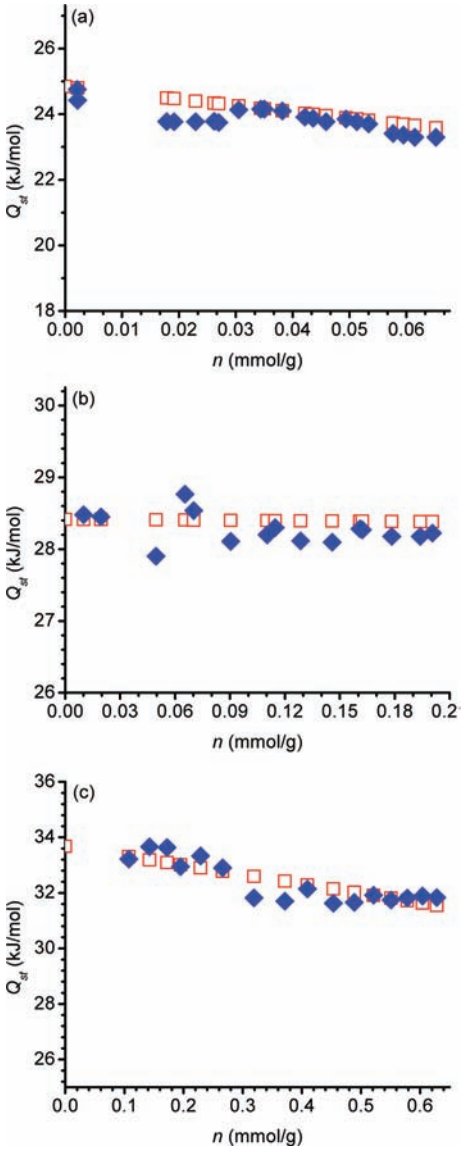

Figure 4. Comparison of the enthalpies for gas adsorption of CH_4 (a), CO_2 (b), and C_2H_2 (c) on **M'MOF-20a** from two methods: linear extrapolation (◆) and virial equation (□).

isosteric enthalpies of adsorption gradually decreased with the increasing surface coverage, while for CO_2, the isosteric enthalpy of adsorption almost remains at 28.4 kJ mol^{-1} within the examined range. As expected, the isosteric enthalpies of adsorption are significantly higher than the enthalpies of vaporization of 8.7, 16.4, and 16.7 kJ mol^{-1} for CH_4, C_2H_2, and CO_2, respectively.[34]

The Henry's law selectivities for CO_2 and C_2H_2 over CH_4 at 295 K, calculated on the basis of the equation $S_{ij} = K_H(i)/K_H(CH_4)$, are 6.8 and 34.9, respectively, both higher than the corresponding values (4.5 and 14.7) in $[Zn_4(OH)_2(1,2,4\text{-}BTC)_2]$.[23c] The C_2H_2/CH_4 selectivity in **M'MOF-20a** is the second highest value ever reported among the porous materials.[23] The CO_2/CH_4 selectivity of 6.8 in **M'MOF-20a** is higher than that of about 3 in a well-examined microporous MOF-508 of the same primitive cubic net for CO_2/CH_4 separation,[25] highlighting the promising potential of **M'MOF-20a** for this industrially important gas separation. The Henry's law selectivities for C_2H_2 over CO_2 in **M'MOF-20a** are 6.2 at 273 K and 5.1 at 295 K, which are higher than those of about 1.0 in $[Zn(dtp)]$[11d] while lower than 12.7 in Mn and Mg formats calculated on the basis of the results from grand-canonical Monte Carlo simulations.[35]

CONCLUSION

In summary, we have successfully synthesized one new microporous mixed metal−organic framework, $Zn_2(BBA)_2(CuPyen)$ (**M'MOF-20a**), of primitive cubic net-work by the metallo-ligand approach. The metallo-ligand approach has secured the immobilization of the accessible open Cu^{2+} sites on the pore surfaces, while the triple framework interpenetration has significantly tuned and reduced the pores to 3.9 Å. The collaborative triple framework interpenetration and the open Cu^{2+} sites induce much stronger interactions with C_2H_2 and CO_2 than CH_4, featuring **M'MOF-20a** as the highly selective microporous M'MOF for the industrially important separation of C_2H_2/CH_4 and CO_2/CH_4. The C_2H_2/CH_4 selectivity of 34.9 on **M'MOF-20a** is the second highest value reported among the porous materials. The uniqueness of the M'MOF approach to systematically tune micropores and immobilize open metal sites to induce their differential interactions with gas molecules has enabled M'MOFs to be promising microporous materials for the adsorptive separation of gas molecules. It is expected that some such microporous M'MOFs will be eventually implemented in the industrial separation of gas molecules in the future.

ASSOCIATED CONTENT

Supporting Information

This material is available free of charge via the Internet at http://pubs.acs.org.

AUTHOR INFORMATION

Corresponding Author

*E-mail: xsc@fjirsm.ac.cn; banglin.chen@utsa.edu.

Notes

The authors declare no competing financial interest.

ACKNOWLEDGMENTS

This work was supported by the Award CHE 0718281 from the NSF and AX-1730 from the Welch Foundation (B.C.). A portion of this research was conducted at the Center for Nanophase Materials Sciences, which is sponsored at Oak Ridge National Laboratory by the Office of Basic Energy Sciences, U.S. Department of Energy.

REFERENCES

(1) (a) Yaghi, O. M.; O'Keeffe, M.; Ockwig, N. W.; Chae, H. K.; Eddaoudi, M.; Kim, J. *Nature* **2003**, *423*, 705. (b) Kitagawa, S.; Kitaura, R.; Noro, S.-I. *Angew. Chem., Int. Ed.* **2004**, *43*, 2334. (c) Férey, G.; Mellot-Draznieks, C.; Serre, C.; Millange, F. *Acc. Chem. Res.* **2005**, *38*, 217. (d) Morris, R. E.; Wheatley, P. S. *Angew. Chem., Int. Ed.* **2008**, *47*, 4966. (e) Ma, L.; Abney, C.; Lin, W. *Chem. Soc. Rev.* **2009**, *38*, 1248. (f) Farha, O. K.; Hupp, J. T. *Acc. Chem. Res.* **2010**, *43*, 1166. (g) Caskey, S. R.; Wong-Foy, A. G.; Matzger, A. J. *J. Am. Chem. Soc.* **2008**, *130*, 10870. (h) Zhao, X.; Xiao, B.; Fletcher, A. J.; Thomas, K. M.; Bradshaw, D.; Rosseinsky, M. J. *Science* **2004**, *306*, 1012. (i) Li,

J.; Kuppler, R. J.; Zhou, H.-C. *Chem. Soc. Rev.* **2009**, *38*, 1477. (j) Murray, L. J.; Dinca, M.; Long, J. R. *Chem. Soc. Rev.* **2009**, *38*, 1294. (k) Ma, S.; Zhou, H. C. *Chem. Commun.* **2010**, *46*, 44. (l) Jiang, H.-L.; Xu, Q. *Chem. Commun.* **2011**, *47*, 3351. (m) Gedrich, K.; Senkovska, I.; Klein, N.; Stoeck, U.; Henschel, A.; Lohe, M. R.; Baburin, I. A.; Mueller, U.; Kaskel, S. *Angew. Chem., Int. Ed.* **2010**, *49*, 8489. (n) Chen, B.; Xiang, S.-C.; Qian, G. *Acc. Chem. Res.* **2010**, *43*, 1115.

(2) Eddaoudi, M.; Kim, J.; Rosi, N.; Vodak, D.; Wachter, J.; O'Keeffe, M.; Yaghi, O. M. *Science* **2002**, *295*, 469.

(3) (a) Vaidhyanathan, R.; Iremonger, S. S.; Dawson, K. W.; Shimizu, G. K. H. *Chem. Commun.* **2009**, 5230. (b) Vaidhyanathan, R.; Iremonger, S. S.; Shimizu, G. K. H.; Boyd, P. G.; Alavi, S.; Woo, T. K. *Science* **2010**, *330*, 650.

(4) (a) An, J.; Fiorella, R. P.; Geib, S. J.; Rosi, N. L. *J. Am. Chem. Soc.* **2009**, *131*, 8401. (b) An, J.; Geib, S. J.; Rosi, N. L. *J. Am. Chem. Soc.* **2010**, *132*, 38.

(5) (a) Maji, T. K.; Uemura, K.; Chang, H.-C.; Matsuda, R.; Kitagawa, S. *Angew. Chem., Int. Ed.* **2004**, *43*, 3269. (b) Horike, S.; Shimomura, S.; Kitagawa, S. *Nat. Chem.* **2009**, *1*, 695.

(6) (a) Zhang, J.-P.; Chen, X.-M. *J. Am. Chem. Soc.* **2009**, *131*, 5516. (b) Zhang, J.-P.; Chen, X.-M. *J. Am. Chem. Soc.* **2008**, *130*, 6010. (c) Zhang, Y.-B.; Zhang, W.-X.; Feng, F.-Y.; Zhang, J.-P.; Chen, X.-M. *Angew. Chem., Int. Ed.* **2009**, *48*, 5287.

(7) (a) Zheng, S.; Li, Y.; Wu, T.; Nieto, R.; Feng, P.; Bu, X. *Chem.—Eur. J.* **2010**, *16*, 13035. (b) Chen, S.; Zhang, J.; Wu, T.; Feng, P.; Bu, X. *J. Am. Chem. Soc.* **2009**, *131*, 16027. (c) Zhang, J.; Wu, T.; Chen, S.-M.; Feng, P.; Bu, X. *Angew. Chem., Int. Ed.* **2009**, *48*, 3486.

(8) Yang, S.; Lin, X.; Blake, A. J.; Walker, G. S.; Hubberstey, P.; Champness, N. R.; Schröder, M. *Nat. Chem.* **2009**, *1*, 487.

(9) Li, K.; Olson, D. H.; Seidel, J.; Emge, T. J.; Gong, H.; Zeng, H.; Li, J. *J. Am. Chem. Soc.* **2009**, *131*, 10368.

(10) Zheng, B.; Bai, J.; Duan, J.; Wojtas, L.; Zaworotko, M. J. *J. Am. Chem. Soc.* **2011**, *133*, 748.

(11) (a) Gücüyener, C.; van den Bergh, J.; Gascon, J.; Kapteijn, F. *J. Am. Chem. Soc.* **2010**, *132*, 17704. (b) Humphrey, S. M.; Chang, J.-S.; Jhung, S. H.; Yoon, J. W.; Wood, P. T. *Angew. Chem., Int. Ed.* **2007**, *46*, 272. (c) Dybtsev, D. N.; Chun, H.; Yoon, S. H.; Kim, D.; Kim, K. *J. Am. Chem. Soc.* **2004**, *126*, 32. (d) Li, J.-R.; Tao, Y.; Yu, Q.; Bu, Z.-H.; Sakamoto, H.; Kitagawa, S. *Chem.—Eur. J.* **2008**, *14*, 2771. (e) Dinca, M.; Long, J. R. *J. Am. Chem. Soc.* **2005**, *127*, 9376. (f) Cheon, Y. E.; Suh, M. P. *Chem. Commun.* **2009**, 2296. (g) Couck, S.; Denayer, J. F. M.; Baron, G. V.; Rémy, T.; Gascon, J.; Kapteijn, F. *J. Am. Chem. Soc.* **2009**, *131*, 6326. (h) Maji, T. K.; Matsuda, R.; Kitagawa, S. *Nat. Mater.* **2007**, *6*, 142. (i) Choi, E.-Y.; Park, K.; Yang, C.- M.; Kim, H.; Son, J.-H.; Lee, S. W.; Lee, Y. H.; Min, D.; Kwon, Y.-U. *Chem.—Eur. J.* **2004**, *10*, 5535. (j) Thallapally, P. K.; Tian, J.; Kishan, M. R.; Fernandez, C. A.; Dalgarno, S. J.; McGrail, P. B.; Warren, J. E.; Atwood, J. L. *J. Am. Chem. Soc.* **2008**, *130*, 16842.

(12) (a) Chen, B.; Liang, C.; Yang, J.; Contreras, D. S.; Clancy, Y. L.; Lobkovsky, E. B.; Yaghi, O. M.; Dai, S. *Angew. Chem., Int. Ed.* **2006**, *45*, 1390. (b) Chen, B.; Ma, S.; Zapata, F.; Lobkovsky, E. B.; Yang, J. *Inorg. Chem.* **2006**, *45*, 5718. (c) Bárcia, P. S.; Zapata, F.; Silva, J. A. C.; Rodrigues, A. E.; Chen, B. *J. Phys. Chem. B* **2007**, *111*, 6101. (d) Chen, B.; Ma, S.; Zapata, F.; Fronczek, F. R.; Lobkovsky, E. B.; Zhou, H.-C. *Inorg. Chem.* **2007**, *46*, 1233. (e) Chen, B.; Ma, S.; Hurtado, E. J.; Lobkovsky, E. B.; Zhou, H. C. *Inorg. Chem.* **2007**, *46*, 8490. (f) Chen, B.; Ma, S.; Hurtado, E. J.; Lobkovsky, E. B.; Liang, C.; Zhu, H.; Dai, S. *Inorg. Chem.* **2007**, *46*, 8705. (g) Das, M. C.; Xu, H.; Xiang, S.-C.; Zhang, Z.-J.; Arman, H. D.; Qian, G.-D.; Chen, B. *Chem.—Eur. J.* **2011**, *17*, 7817. (h) He, Y.; Zhang, Z.; Xiang, S.; Fronczek, F. R.; Krishna, R.; Chen, B. *Chem.—Eur. J.* **2012**, *18*, 613. (i) He, Y.; Zhang, Z.; Xiang, S.; Wu, H.; Fronczek, F. R.; Zhou, W.; Krishna, R.; O'Keeffe, M.; Chen, B. *Chem.—Eur. J.* **2012**, *18*, 1901.

(13) (a) Dietzel, P. D. C.; Morita, Y.; Blom, R.; Fjellvag, H. *Angew. Chem., Int. Ed.* **2005**, *44*, 6354. (b) Rosi, N. L.; Kim, J.; Eddaoudi, M.; Chen, B.; O'Keeffe, M.; Yaghi, O. M. *J. Am. Chem. Soc.* **2005**, *127*, 1504. (c) Dietzel, P. D. C.; Panella, B.; Hirscher, M.; Blom, R.; Fjellvag, H. *Chem. Commun.* **2006**, 959. (d) Dietzel, P. D. C.; Johnsen, R. E.; Blom, R.; Fjellvag, H. *Chem.—Eur. J.* **2008**, *14*, 2389. (e) Vitillo, J. G.; Regli, L.; Chavan, S.; Ricchiardi, G.; Spoto, G.; Dietzel, P. D. C.; Bordiga, S.; Zecchina, A. *J. Am. Chem. Soc.* **2008**, *130*, 8386. (f) Dietzel, P. D. C.; Johnsen, R. E.; Fjellvag, H.; Bordiga, S.; Groppo, E.; Chavan, S.; Blom, R. *Chem. Commun.* **2008**, 5125.

(14) (a) McKinlay, A. C.; Xiao, B.; Wragg, D. S.; Wheatley, P. S.; Megson, I. L.; Morris, R. E. *J. Am. Chem. Soc.* **2008**, *130*, 10440. (b) Zhou, W.; Wu, H.; Yildirim, T. *J. Am. Chem. Soc.* **2008**, *130*, 15268. (c) Wu, H.; Zhou, W.; Yildirim, T. *J. Am. Chem. Soc.* **2009**, *131*, 4995. (d) Liu, Y.; Kabbour, H.; Brown, C. M.; Neumann, D. A.; Ahn, C. C. *Langmuir* **2008**, *24*, 4772. (e) Britt, D.; Furukawa, H.; Wang, B.; Glover, T. G.; Yaghi, O. M. *Proc. Natl. Acad. Sci. U. S. A.* **2009**, *106*, 20637. (f) Xiang, S. C.; Zhou, W.; Zhang, Z. J.; Green, M. A.; Liu, Y.; Chen, B. *Angew. Chem., Int. Ed.* **2010**, *49*, 4615. (g) Gadipelli, S.; Ford, J.; Zhou, W.; Wu, H.; Udovic, T. J.; Yildirim, T. *Chem.—Eur. J.* **2011**, *17*, 6043. (h) Yazaydın, A. ö.; Snurr, R. Q.; Park, T.-H.; Koh, K.; Liu, J.; LeVan, M. D.; Benin, A. I.; Jakubczak, P.; Lanuza, M.; Galloway, D. B.; Low, J. J.; Willis, R. R. *J. Am. Chem. Soc.* **2009**, *131*, 18198−18199.

(15) (a) Lin, X.; Telepeni, I.; Blake, A. J.; Dailly, A.; Brown, C. M.; Simmons, J. M.; Zoppi, M.; Walker, G. S.; Thomas, K. M.; Mays, T. J.; Hubberstey, P.; Champness, N. R.; Schröder, M. *J. Am. Chem. Soc.* **2009**, *131*, 2159. (b) Wang, X.-S.; Ma, S.; Forster, P. M.; Yuan, D.; Eckert, J.; Lopez, J. J.; Murphy, B. J.; Parise, J. B.; Zhou, H.-C. *Angew. Chem., Int. Ed.* **2008**, *47*, 7263. (c) Yuan, D.; Zhao, D.; Sun, D.; Zhou, H.-C. *Angew. Chem., Int. Ed.* **2010**, *49*, 5357. (d) Lee, Y.-G.; Moon, H. R.; Cheon, Y. E.; Suh, M. P. *Angew. Chem., Int. Ed.* **2008**, *47*, 7741. (e) Ma, L.; Lin, W. *Angew. Chem., Int. Ed.* **2009**, *48*, 3637. (f) Chen, B.; Ockwig, N. W.; Millward, A. R.; Contreras, D. S.; Yaghi, O. M. *Angew. Chem., Int. Ed.* **2005**, *44*, 4745. (g) Hu, Y.-X.; Xiang, S.-C.; Zhang, W.-W.; Zhang, Z.-X.; Wang, L.; Bai, J.-F.; Chen, B. *Chem. Commun.* **2009**, *45*, 7551. (h) Xiang, S. C.; Zhou, W.; Gallegos, J. M.; Liu, Y.; Chen, B. *J. Am. Chem. Soc.* **2009**, *131*, 12415. (i) Guo, Z.-Y.; Wu, H.; Srinivas, G.; Zhou, Y.-M.; Xiang, S.-C.; Chen, Z.-X.; Yang, Y.-T.; Zhou, W.; O'Keeffe, M.; Chen, B. *Angew. Chem., Int. Ed.* **2011**, *50*, 3178.

(16) (a) Choi, H.-S.; Suh, M. P. *Angew. Chem., Int. Ed.* **2009**, *48*, 6865. (b) Chen, B.; Yang, Y.; Zapata, F.; Lin, G.; Qian, G.-D.; Lobkovsky, E. B. *Adv. Mater.* **2007**, *19*, 1693. (c) Zhou, W.; Yildirim, T. *J. Phys. Chem. C* **2008**, *112*, 8132. (d) Dinca, M.; Long, J. R. *Angew. Chem., Int. Ed.* **2008**, *47*, 6766.

(17) (a) Kitaura, R.; Onoyama, G.; Sakamoto, H.; Matsuda, R.; Noro, S.-I.; Kitagawa, S. *Angew. Chem., Int. Ed.* **2004**, *43*, 2684. (b) Chen, B.; Fronczek, F. R.; Maverick, A. W. *Inorg. Chem.* **2004**, *43*, 8209. (c) Cho, S.-H.; Ma, B.; Nguyen, S. T.; Hupp, J. T.; Albrecht-Schmitt, T. E. *Chem. Commun.* **2006**, 2563. (d) Song, F.; Wang, C.; Falkowski, J. M.; Ma, L.; Lin, W. *J. Am. Chem. Soc.* **2010**, *132*, 15390. (e) Das, M. C.; Xiang, S.-C.; Zhang, Z.-J.; Chen, B. *Angew. Chem., Int. Ed.* **2011**, *50*, 10510.

(18) (a) Rowsell, J. L. C.; Yaghi, O. M. *J. Am. Chem. Soc.* **2006**, *128*, 1304. (b) Jagiello, J.; Bandosz, T. J.; Putyera, K.; Schwarz, J. A. *J. Chem. Eng. Data* **1995**, *40*, 1288. (c) Xiang, S.; Zhang, Z.; Zhao, C.-G.; Hong, K.; Zhao, X.; Ding, D.-R.; Xie, M.-H.; Wu, C.-D.; Das, M. C.; Gill, R.; Thomas, K. M.; Chen, B. *Nat. Commun.* **2011**, *2*, 204. (d) Chen, B.; Zhao, X.; Putkham, A.; Hong, K.; Lobkovsky, E. B.; Hurtado, E. J.; Fletcher, A. J.; Thomas, K. M. *J. Am. Chem. Soc.* **2008**, *130*, 6411. (e) Zhao, V.-R.; Fletcher, A. J.; Thomas, K. M. *J. Phys. Chem. B* **2006**, *110*, 9947.

(19) (a) Rigaku Mercury CCD diffractometer: Rigaku. *CrystalClear*, version 1.35; Rigaku Corp.: Tokyo, Japan, 2001. (b) Rigaku AFC7R diffractometer: Rigaku. *CrystalStructure*, version 3.10; Rigaku Corp. and Rigaku/MSC: Tokyo, Japan, 2002.

(20) Spek, L. *PLATON*: The University of Utrecht: Utrecht, The Netherlands, 1999.

(21) *CRC Handbook of Chemistry and Physics*, 74th ed.; The Chemical Rubber Co.: Boca Raton, FL, 1993.

(22) Reid, C. R.; Thomas, K. M. *J. Phys. Chem. B* **2001**, *105*, 10619.

(23) (a) Zhang, Z.-J.; Xiang, S.-C.; Chen, B. *CrystEngComm* **2011**, *13*, 5983. (b) Zhang, Z.-J.; Xiang, S.; Chen, Y.-S.; Ma, S.; Lee, Y.; Phely-Bobin, T.; Chen, B. *Inorg. Chem.* **2010**, *49*, 8444. (c) Zhang, Z.-J.; Xiang, S.-C.; Rao, X.-T.; Zheng, Q.; Fronczek, F. R.; Qian, G.-D.; Chen, B. *Chem. Commun.* **2010**, *46*, 7205. (d) Chen, Z.-X.; Xiang, S.-

C.; Arman, H. D.; Zhao, D.-Y.; Chen, B. *Eur. J. Inorg. Chem.* **2010**, 3745. (e) Chen, Z.-X.; Xiang, S.-C.; Arman, H. D.; Mondal, J. U.; Li, P.; Zhao, D.-Y.; Chen, B. *Inorg. Chem.* **2011**, *50*, 3442.
(24) (a) Li, J.-R.; Ma, Y.; McCarthy, M. C.; Sculley, J.; Yu, J.; Jeong, H.-K.; Balbuena, P. B.; Zhou, H.-C. *Coord. Chem. Rev.* **2011**, *255*, 1791. (b) Du, N.; Park, H. B.; Robertson, G. P.; Dal-Cin, M. M.; Visser, T.; Scoles, L.; Guiver, M. D. *Nat. Mater.* **2011**, *10*, 372. (c) Si, X.; Jiao, C.; Li, F.; Zhang, J.; Wang, S.; Liu, S.; Li, Z.; Sun, L.; Xu, F.; Gabelica, Z.; Schick, C. *Energy Environ. Sci.* **2011**, DOI: 10.1039/c1ee01380g.. (d) Simmons, J. M.; Wu, H.; Zhou, W.; Yildirim, T. *Energy Environ. Sci.* **2011**, *4*, 2177. (e) D'Alessandro, D. M.; Smit, B.; Long, J. R. *Angew. Chem., Int. Ed.* **2010**, *49*, 6058.
(25) Bastin, L.; Barcia, P. S.; Hurtado, E. J. J.; Silva, A. C.; Rodrigues, A. E.; Chen, B. *J. Phys. Chem. C* **2008**, *112*, 1575.
(26) Yao, S.; Nakayama, A.; Suzuki, E. *Catal. Today* **2001**, *71*, 219.
(27) Bullerwell, J.; Kenchenpur, A.; Whidden, T. K. *Fuel* **2010**, *89*, 254.
(28) Fasuer, G. U.S. Patent 2894602, 1959.
(29) Nayak, V. S. *J. Chromatogr. A* **1991**, *556*, 425.
(30) Newalkar, B. L.; Choudary, N. V.; Kumar, P.; Komarneni, S.; Bhat, T. S. G. *Chem. Mater.* **2002**, *14*, 304.
(31) Reid, C. R.; Thomas, K. M. *Langmuir* **1999**, *15*, 3206.
(32) Llewellyn, P. L.; Bourrelly, S.; Serre, C.; Vimont, A.; Daturi, M.; Hamon, L.; DeWeireld, G.; Chang, J.-S.; Hong, D.-Y.; Hwang, Y. K.; Jhung, S. H.; Ferey, G. *Langmuir* **2008**, *24*, 7245.
(33) Demessence, A.; D'Alessandro, D. M.; Foo, M. L.; Long, J. R. *J. Am. Chem. Soc.* **2009**, *131*, 8784.
(34) Chickos, J. S.; Acree, W. E. *J. Phys. Chem. Ref. Data* **2003**, *32*, 519.
(35) Fischer, M.; Hoffmann, F.; Froba, M. *ChemPhysChem* **2010**, *11*, 2220.